Designing Silicon-Germanium Photodetectors with Numerical Optimization: The Tradeoffs and Limits

Ergun Simsek and Curtis R. Menyuk

University of Maryland Baltimore County, Baltimore, MD 21250, USA.

ABSTRACT

We initially developed an efficient solver to study photodetectors composed of multiple semiconductor layers with varying thicknesses and doping concentrations. Subsequently, we employed it as the forward solver for three different numerical optimization methods aimed at designing Si-Ge photodetectors with larger bandwidth, higher quantum efficiency, and lower phase noise. Our work offers new insights into the design of high-performance photodetectors—a challenging task due to computation time, design constraints, and the complexity of estimating sensitivity to design parameters.

Keywords: photodiodes, photodetectors, numerical optimization, quantum efficiency, phase noise, bandwidth.

1. INTRODUCTION

With its compatibility for monolithic integration with silicon and its higher electron and hole mobilities compared to silicon, germanium is an essential semiconductor to be used in photonic devices—including photodetectors.[1] However, designing a high-performance photodetector or even improving the performance of an already existing design is a challenging task due to the required computation time, difficulties in estimating the sensitivity of the device to the design parameters, and the existence of design constraints.[2–4] To overcome this challenge, we recently developed an efficient drift-diffusion equations solver that uses a non-uniform time-stepping[5] and both single-frequency and broadband excitations[6] to study photodetectors that have several layers of semiconducting materials with varying thicknesses and doping concentrations. With this numerical solver, we can calculate photodetectors' phase noise, quantum efficiency, and response time to estimate their stability, efficiency, and speed.

In this work, we use three different numerical optimization methods (NOMs): genetic algorithm (GA), surrogate algorithm (SA), and particle swarm optimization (PSO) algorithm to design Si-Ge photodetectors with a higher quantum efficiency, wider bandwidth, and lower phase noise. The analysis of the 1800 designs with uniform doping and 2800 designs with gradient doping generated during the numerical optimization studies leads to several findings as discussed below.

2. METHODS

We solve the following equations

$$\begin{aligned}\frac{\partial(p-N_A^-)}{\partial t} &= -\frac{1}{q}\nabla\cdot\mathbf{J}_p + G_{\text{ii}} + G_{\text{opt}} - R(n,p),\\ \frac{\partial(n-N_D^+)}{\partial t} &= +\frac{1}{q}\nabla\cdot\mathbf{J}_n + G_{\text{ii}} + G_{\text{opt}} - R(n,p),\\ \nabla\ \cdot\ \mathbf{E} &= \frac{q}{\epsilon}\left(n-p+N_A^- - N_D^+\right),\end{aligned} \tag{1}$$

using finite differences, where n is the electron density, p is the hole density, t is time, q is the unit of charge, $\mathbf{J}_n$ is the electron current density, $\mathbf{J}_p$ is the hole current density, R is the recombination rate, G_{ii} and G_{opt} are

Further author information: (Send correspondence to E.S.) E-mail: simsek@umbc.edu, Telephone: +1 410 455 3540.

impact ionization and optical generation rates, $\mathbf{E}$ is the electric field at any point in the device, ϵ is the electrical permittivity, N_A^- is the ionized acceptor concentration, and N_D^+ is the ionized donor concentration. The electron and hole current densities are described with $\mathbf{J}_p = qp\mathbf{v}_p(\mathbf{E}) - qD_p\nabla p$ and $\mathbf{J}_n = qn\mathbf{v}_n(\mathbf{E}) + qD_n\nabla n$, where $\mathbf{v}_n(\mathbf{E})$ and $\mathbf{v}_p(\mathbf{E})$ are the electric-field-dependent electron and hole drift velocities, D_n and D_p are the electron and hole diffusion coefficients, respectively. We use the following empirical expressions for $\mathbf{v}_n(\mathbf{E})$ and $\mathbf{v}_p(\mathbf{E})$ to fit the measured results

$$\mathbf{v}_n(\mathbf{E}) = \frac{\mathbf{E}\left(\mu_n + v_{n,\text{sat}}\beta|\mathbf{E}|\right)}{1+\beta|\mathbf{E}|^2} \qquad \text{and} \qquad \mathbf{v}_p(\mathbf{E}) = \frac{\mu_p v_{p,\text{sat}}\mathbf{E}}{\left(v_{p,\text{sat}}^{\gamma} + \mu_p^{\gamma}|\mathbf{E}|^{\gamma}\right)^{1/\gamma}}, \tag{2}$$

where μ_n is the electron low-field mobility, $v_{n,\text{sat}}$ is the saturated electron velocity, β is a fitting parameter, μ_p is the hole low-field mobility, γ is an empirical fitting parameter that depends on temperature, and $v_{p,\text{sat}}$ is the saturated hole velocity. To take into account the dependence of electron and hole low field mobilities, μ_n and μ_p, on the doping density, we define

$$\mu_{n,p} = \frac{\mu_{n_0,p_0}}{1+\left(\dfrac{N_D+N_A}{N_{\text{ref}}}\right)^{\eta}}, \tag{3}$$

where μ_{n_0} and μ_{p_0} are electron and hole mobilities at low doping concentrations, respectively, while N_{ref} and η are empirical parameters. The electric field dependent electron and hole diffusion coefficients are calculated with[2]

$$D_n(\mathbf{E}) = \frac{k_B T\mu_n/q}{\left[1-2\left(|\mathbf{E}|/E_p\right)^2 + \frac{4}{3}\left(|\mathbf{E}|/E_p\right)^3\right]^{1/4}} \qquad \text{and} \qquad D_p(\mathbf{E}) = \frac{k_B T}{q}\frac{\mathbf{v}_p(\mathbf{E})}{\mathbf{E}}, \tag{4}$$

where E_p is the electric field at which the diffusion constant peaks. The main contribution to the recombination rate in Eq. (1) is the Shockley-Read-Hall (SRH) effect, which yields[7]

$$R = \frac{np - n_i^2}{\tau_p(n+n_i) + \tau_n(p+n_i)}, \tag{5}$$

where τ_n, τ_p, and n_i are the electron and hole lifetimes and intrinsic carrier density respectively.

The optical generation rate in Eq. (1) is $G_{\text{opt}}(x,t) = G_c(t)e^{-\alpha(L-x)}$, where α is the absorption coefficient, x is distance across the device, L is the device length, and $G_c(t)$ is the generation rate coefficient as a function of time, which is given by $G_c(t) = \alpha P_{\text{opt}}(t)/AW_{\text{photon}}$, where $P_{\text{opt}}(t)$ is the optical power as a function of time, A is the area of the light spot, and W_{photon} is the photon energy.[8] Note that the generation rate in the absorption layer depends on the location in the device as well as the material. The total output current is the sum of the hole, electron, and displacement currents, i.e. $J_{\text{total}} = J_n + J_p + \epsilon\partial E/\partial t$.

Our model accounts for the incomplete ionization of doping impurities such as boron, aluminum, and nitrogen, using the following expressions,[8,9]

$$\begin{aligned} N_D^+ &= \frac{N_D}{1+g_D\exp\left(\dfrac{E_C-E_D}{k_BT}\right)\exp\left(\dfrac{E_{Fn}-E_C}{k_BT}\right)}, \\ N_A^- &= \frac{N_A}{1+g_A\exp\left(\dfrac{E_A-E_V}{k_BT}\right)\exp\left(-\dfrac{E_{Fp}-E_V}{k_BT}\right)}, \end{aligned} \tag{6}$$

where N_D and N_A are the donor and acceptor impurity concentrations, g_D and g_A are the respective ground-state degeneracy of donor and accept impurity levels,[4,10] E_A and E_D are the acceptor and donor energy levels, E_C and E_V are the low conduction band and the high valence band energy levels, E_{Fn} and E_{Fp} are the quasi-Fermi energy levels for the electrons and holes, and T is the temperature. The electron and hole generation rate due to impact ionization G_{ii} are given by $G_{\text{ii}} = (\alpha_n|\mathbf{J}_n| + \alpha_p|\mathbf{J}_p|)/q$, where α_n and α_p are the impact ionization

coefficients of the electrons and holes, respectively.[11] We calculate their values with $\alpha_n = A_n \cdot e^{-B_n/|\mathbf{E}|}$ and $\alpha_p = A_p \cdot e^{-B_p/|\mathbf{E}|}$, where A_n, B_n, A_p, and B_p are experimentally-determined parameters.[11–13]

The semiconductor materials are defined using 34 parameters.[14] The implicit Euler method is used to discretize the drift-diffusion equations in time t for numerical computation. The spatial discretization along x is done non-uniformly, so that the spatial sampling density increases near the interfaces between neighboring layers. We also utilize a nonuniform time-stepping method[5] that uses large time steps when the fields and current are not significantly changing inside the domain of interest and uses smaller time steps when they are expected to change (i.e., near the pulse center). This approach dramatically reduces the number of time steps used for the dynamic analysis.[5]

To verify the accuracy of this solver, we first study an experimentally characterized Si-Ge photodetector,[1] shown in Fig. 1(a). The 0.6-μm Ge layer has a doping density that is graded from 5×10^{19} cm^{-3} to 2×10^{17} cm^{-3} as illustrated in Fig. 1(b). In Figs. 1(c)-(f), we plot different features of this photodetector that are calculated with our solver. Fig. 1(g) shows the good agreement between the measurement[1] and our numerical results for the RF output power of the photodetector under the reverse bias of 5 V.

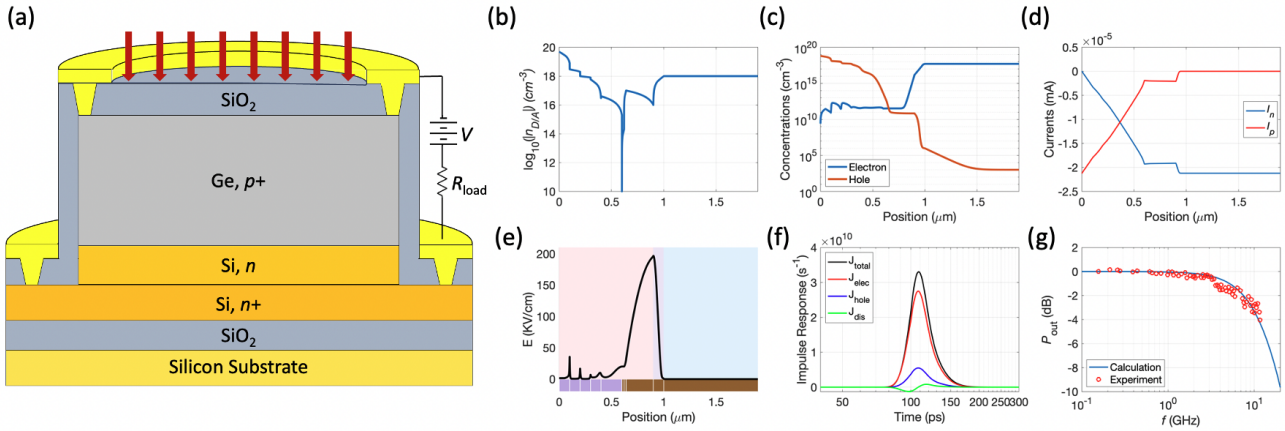

Figure 1. (a) Schematic view of the silicon-germanium (Si-Ge) photodetector cross-section with $p+$ Ge, n Si, and $n+$ Si layers fabricated on top of a SiO_2 coated Si-substrate. (a) Doping concentration of the Si-Ge photodetector that is experimentally studied in.[1] The calculated values for (c) charge, (d) current, (e) electric field distributions along the photodetector. (f) Impulse response of the device. (g) RF output power: numerical (blue curve) vs. experimental values (red circles).

3. NUMERICAL OPTIMIZATION

We use three different numerical optimization methods (NOMs): genetic algorithm (GA), surrogate algorithm (SA), and particle swarm optimization (PSO) algorithm to design photodetectors with a higher quantum efficiency, wider bandwidth, and a lower phase noise. The thicknesses and doping concentrations of each layer ($p+$ Ge, n Si, and $n+$ Si) are left to be determined by the NOMs.

For all the calculations, we assume that the photodetector is reverse-biased ($V = -5$ V) and is illuminated by a continuous wave laser operation at 1550 nm. The diameters of the incident beam and photodetector are both 15 μm. The load resistance is 50 Ω. The phase noise is calculated at 0.5 GHz.

First, we assume that each layer has a uniform doping concentration. The $p+$ and $n+$ layers' doping concentration can be any value between 10^{16} cm^{-3} and 10^{20} cm^{-3}, while the n-layer's doping concentration range is 10^{12} cm^{-3} – 10^{16} cm^{-3}. The minimum and maximum thickness values for each layer are 10 nm and 1 μm, respectively. For the second set of numerical optimization study, we allow the doping concentrations to change gradually within each layer, again within the aforementioned ranges.

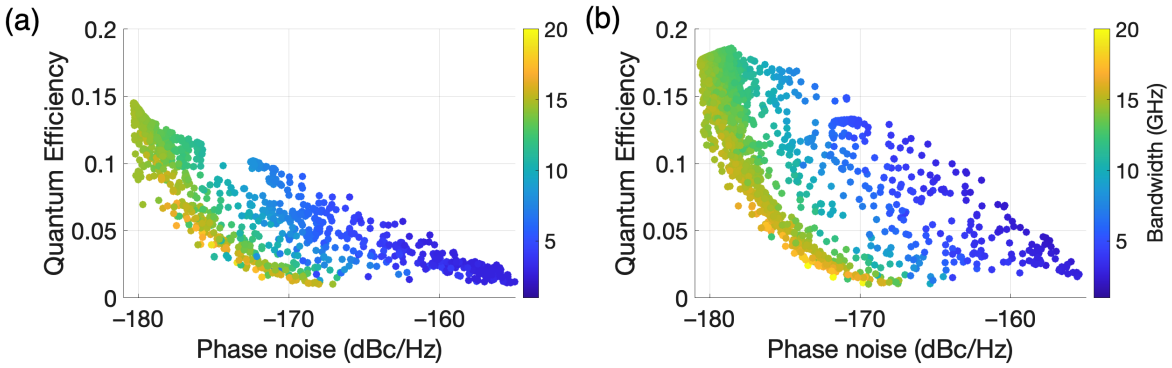

Figure 2. Each circle represents the phase noise and quantum efficiency of a unique photodetector design assuming a (a) uniform-doping and (b) gradient-doping. The filling color changes from dark blue to yellow, corresponding to the bandwidth of the photodetector.

In Fig. 2, each circle one unique design's phase noise and quantum efficiency values assuming (a) uniform doping concentration in each layer and (b) gradient-doping, respectively. For both cases, we observe that (i) the photodetectors with lower phase noise are likely to have a higher quantum efficiency and wider bandwidth, and (ii) the photodetectors with a gradient-doping can have a higher quantum efficiency (0.18 vs. 0.14) compared to the ones with uniform doping concentrations. When we investigate the electric field profiles along these photodetectors, we observe that gradient (decreasing) doping density levels in the absorber and collection layers improves the quantum efficiency by increasing the width of the depletion region and suppressing the Auger mechanism.

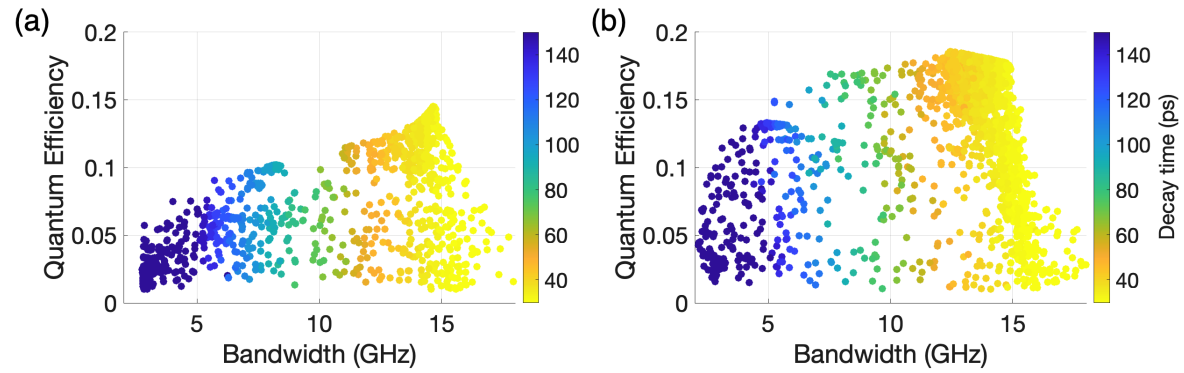

Figure 3. Follows Fig. 2 for bandwidth vs. quantum efficiency and filling color represents the decay time of the pulses along the devices.

Figure 3 is similar to the Fig. 2 but here the $x-$axis is the bandwidth of the photodetectors and the colors changing from yellow (fast) to dark blue (slow) represent their decay time, where the decay time refers to the time it takes for the photodetector's output signal to decrease to 1% of its maximum value after the incident light has been removed or turned off. In term of bandwidth, the gradient doping does not bring an obvious advantage but Fig. 3(b) shows that if we enlarge our optimization search domain, we might obtain designs that have quantum efficiency close to 0.2. However, for the uniform doping concentration, the maximum possible quantum efficiency is approximately 0.15.

Note that increasing the number of layers allows us to obtain designs with larger bandwidths.[15] In these designs, we observe that the intrinsic layer should be neither too thin nor too thick. Our general guidelines for designing a photodetector with a large bandwidth, high quantum efficiency, and low phase noise are as follows: (i) the thickness of the $n+$ layer should be as high as possible; (ii) the thickness of the i-layer should

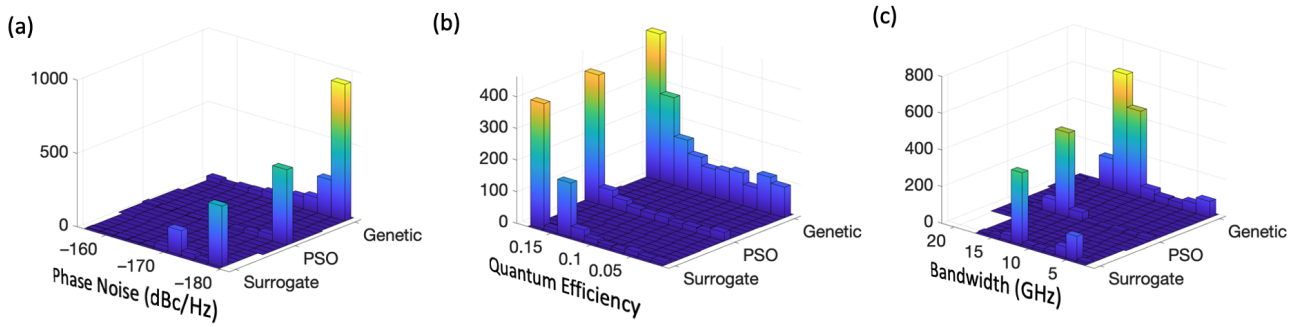

Figure 4. Histogram plots for (a) phase noise, (b) quantum efficiency, and (c) bandwidth for the photodetectors with gradient-doping concentrations that are designed with the surrogate optimization, particle-swarm optimization (PSO), and genetic optimization algorithms.

be optimized to balance trade-offs between quantum efficiency, bandwidth, and phase noise; (iii) rather than doping concentrations alone, the doping concentrations normalized with the layer thickness have a more profound impact on the performance parameters, and (iv) the gradient-doping concentration profiles, especially in the $p+$ and i-regions, need to be determined through numerical optimization.

Figures 4 (a)-(c) display the histogram analysis for phase noise, quantum efficiency, and bandwidth, respectively, of the photodetectors with gradient-doping concentrations designed using surrogate optimization, particle-swarm optimization (PSO), and genetic optimization algorithms. Overall, all of the optimization methods succeeded in creating designs that met the initial design goals (quantum efficiency ¿ 0.18, bandwidth ¿ 15 GHz, and phase noise < -178 dBc/Hz). However, there were differences in the number of iterations required to reach these goals. In this regard, the genetic algorithm was slower compared to the other two methods employed. Due to its combinatorial nature, the genetic algorithm also generated a significant number of designs with low quantum efficiencies. When considering the iteration time and the number of highly successful designs compared to all the trials, the PSO can be considered the optimum choice among these three methods for this small-scale optimization problem. Another recent study of ours shows that for numerical optimization studies with a higher number of parameters to be optimized, the surrogate optimization method can outperform the PSO and genetic algorithms.[15]

4. CONCLUSION

This work presents a numerical investigation into the impact of doping concentrations and thicknesses of photodetectors on their quantum efficiency, phase noise, and bandwidth. Our analysis reveals that (i) the quantum efficiency $\times$ bandwidth increases with decreasing phase noise, (ii) photodetectors with gradient-doping profiles can have a higher quantum efficiency due to the increased width of the depletion region and suppressed Auger mechanism, and (iii) for a given number of layers and material types, we can identify the upper limits for the highest achievable quantum efficiency and lowest phase noise numerically.

ACKNOWLEDGMENTS

The authors acknowledge support from the Naval Research Laboratory (Award no. N00173-21-1-G901).

REFERENCES

[1] Li, C., Xue, C. L., Liu, Z., Cong, H., Cheng, B., Hu, Z., Guo, X., and Liu, W., "High-responsivity vertical-illumination Si/Ge uni-traveling-carrier photodiodes based on silicon-on-insulator substrate," *Scientific Reports* **6**, 27743, (2016).

[2] Williams, K. J., [Microwave nonlinearities in photodiodes], PhD Dissertation, University of Maryland College Park, Maryland, USA (1994).

[3] Mahabadi, S. E. J., Wang, S., Carruthers, T. F., Menyuk, C. R., Quinlan, F. J., Hutchinson, M. N., McKinney, J. D., and Williams, K. J., "Calculation of the impulse response and phase noise of a high-current photodetector using the drift-diffusion equations," *Opt. Express* **27**(3), 3717–3730 (2019).

[4] Hu, Y., Marks, B. S., Menyuk, C. R., Urick, V. J., and Williams, K. J., "Modeling sources of nonlinearity in a simple p-i-n photodetector," *J. Lightwave Technol.* **32**, 3710–3720 (2014).

[5] Simsek, E., Anjum, I. Md, Carruthers, T. F., and Menyuk, C. R., "Non-Uniform Time-Stepping For Fast Simulation of Photodetectors Under High-Peak-Power, Ultra-Short Optical Pulses," 22$^{\text{nd}}$ Int. Conf. on Num. Sim. of Optoelec. Dev. (2022).

[6] Simsek, E., Anjum, I. Md, Carruthers, T. F., Menyuk, C. R., Campbell, J. C., Tulchinsky, D. A., and Williams, K. J, "Fast Evaluation of RF Power Spectrum of Photodetectors with Windowing Functions," *IEEE Trans. on Electron Devices* **70** (7), 3643–3648 (2023).

[7] Razeghi, M., [Fundamentals of Solid State Engineering], Springer (2006).

[8] Hu, Y., [Modeling Nonlinearity and Noise in High-Current Photodetectors], Ph.D. Dissertation, University of Maryland, Baltimore County, Maryland, USA (2017).

[9] Scaburri, R., [The incomplete ionization of substitutional dopants in Silicon Carbide], PhD Dissertation, University of Bologna, Bologna, Italy (2011).

[10] Xiao, G., Lee, J., Lioua, J.J., and Ortiz-Conde, A., "Incomplete ionization in a semiconductor and its implications to device modeling," *Microelectron. Reliab.* **39**, 1299–1303 (1999).

[11] Selberherr, S., [Analysis and Simulation of Semiconductor Devices], Springer (2012).

[12] Yang, K., Cowles, J. C., East, J. R., and Haddad, G. I., "Theoretical and experimental dc characterization of InGaAs-based abrupt emitter HBT's," *IEEE Trans. Electron Devices* **42**, 1047–1058 (1995).

[13] Wang H. and Ng, G.-I., "Avalanche multiplication in InP/InGaAs double heterojunction bipolar transistors with composite collectors," *IEEE Trans. Electron Devices* **47**, 1125–1133 (2000).

[14] Simsek, E., Anjum, I. Md, and Menyuk, C. R., "Solving Drift Diffusion Equations on Non-uniform Spatial and Temporal Domains,"44th PhotonIcs and Electromagnetics Research Symposium (PIERS), Prague, Czechia, July 3–6, 2023.

[15] Islam, R., Anjum, I. Md, Menyuk, C. R., and Simsek, E., "Designing Silicon-Germanium Photodetectors with Numerical Optimization: The Tradeoff Between Quantum Efficiency and Phase Noise," 2023 Conference on Lasers and Electro-Optics/Europe – European Quantum Electronics Conferences (CLEO/Europe-EQEC 2023), Munich, Germany (2023).